Phosphatidylinositol 3,5-bisphosphate regulates the transition between *trans*-SNARE complex formation and vacuole membrane fusion

Gregory E. Miner[a], Katherine D. Sullivan[a], Annie Guo[a], Brandon C. Jones[a], Logan R. Hurst[a], Ez C. Ellis[a], Matthew L. Starr[a], and Rutilio A. Fratti[a,b,*]
[a]Department of Biochemistry and [b]Center for Biophysics and Quantitative Biology, University of Illinois at Urbana–Champaign, Urbana, IL 61801

ABSTRACT Phosphoinositides (PIs) regulate a myriad of cellular functions including membrane fusion, as exemplified by the yeast vacuole, which uses various PIs at different stages of fusion. In light of this, the effect of phosphatidylinositol 3,5-bisphosphate ($PI(3,5)P_2$) on vacuole fusion remains unknown. $PI(3,5)P_2$ is made by the PI3P 5-kinase Fab1 and has been characterized as a regulator of vacuole fission during hyperosmotic shock, where it interacts with the TRP Ca^{2+} channel Yvc1. Here we demonstrate that exogenously added dioctanoyl (C8) $PI(3,5)$ P_2 abolishes homotypic vacuole fusion. This effect was not linked to Yvc1, as fusion was equally affected using *yvc1Δ* vacuoles. Thus, the effects of C8-$PI(3,5)P_2$ on fusion and fission operate through distinct mechanisms. Further testing showed that C8-$PI(3,5)P_2$ inhibited vacuole fusion after *trans*-SNARE pairing. Although SNARE complex formation was unaffected, we found that C8-$PI(3,5)P_2$ blocked outer leaflet lipid mixing. Overproduction of endogenous $PI(3,5)P_2$ by the *fab1[T2250A]* hyperactive kinase mutant also inhibited the lipid mixing stage, bolstering the model in which $PI(3,5)P_2$ inhibits fusion when present at elevated levels. Taken together, this work identifies a novel function for $PI(3,5)P_2$ as a regulator of vacuolar fusion. Moreover, it suggests that this lipid acts as a molecular switch between fission and fusion.

INTRODUCTION

The ability of lipids, and specifically phosphoinositides (PIs), to regulate membrane homeostasis has been well established. Classically, PI-dependent regulation is associated with the recruitment of soluble proteins to membranes to promote the proteins' function. However, a growing body of work now shows that PIs and other regulatory lipids contribute to a wide array of functions including transcriptional regulation (Carman and Han, 2009), protein sequestering to inhibit function (Starr *et al.*, 2016), microdomain formation

(Simons and Toomre, 2000; Fratti *et al.*, 2004), modulating the physical properties of membranes (Andersen and Koeppe, 2007; Zick *et al.*, 2014), and regulating the activity of membrane-anchored proteins (Dong *et al.*, 2010; Li *et al.*, 2014; Kiontke *et al.*, 2017). The rapid modification of lipids by specific kinases, phosphatases, and lipases adds an additional layer of complexity by affecting the spatiotemporal control of cellular events. In the context of *Saccharomyces cerevisiae* vacuole homeostasis, two of the important PIs are PI3P and $PI(3,5)P_2$. These lipids appear to play opposing roles, as PI3P is characterized as a positive regulator of fusion (Boeddinghaus *et al.*, 2002; Fratti *et al.*, 2004; Karunakaran and Fratti, 2013; Lawrence *et al.*, 2014), whereas $PI(3,5)P_2$ promotes vacuolar fission (Gary *et al.*, 1998; Bonangelino *et al.*, 2002).

$PI(3,5)P_2$ is found predominantly in the late endosome and vacuole, where it is made exclusively by the PI3P 5-kinase Fab1 (Yamamoto *et al.*, 1995; Gary *et al.*, 1998). Deletion of *FAB1* results in a complete loss of $PI(3,5)P_2$, as well as a drastic enlargement of the vacuole. $PI(3,5)P_2$ can be dephosphorylated to PI3P by the $PI(3,5)P_2$ 5-phosphatase Fig4 (Gary *et al.*, 2002), yet the deletion of *FIG4* leads to an overall decrease in $PI(3,5)P_2$ (Duex *et al.*, 2006a,b; Efe *et al.*, 2007). This is due to the required presence of Fig4 along

FIGURE 1: Dioctanoyl lipids and vacuole homotypic fusion. WT (A) or *yvc1Δ* (B) vacuoles were tested for fusion with buffer alone or a dose-response curve of C8-PI(3,5)P$_2$. (C) WT vacuole fusion in the presence of C8-PI3P. (D) WT vacuole fusion in the presence of C8-PI(3,5)P$_2$ or C8-PI(4,5)P$_2$. Error bars are SEM ($n = 3$). **$p < 0.01$, ***$p < 0.001$ (unpaired *t* test).

with Vac7, Vac14, and Atg18 in the Fab1 complex to yield maximum activity (Sbrissa *et al.*, 2007; Botelho *et al.*, 2008; Jin *et al.*, 2008).

The enlarged vacuolar phenotype seen with the loss of Fab1 suggested a role for PI(3,5)P$_2$ in membrane fission. Further work showed that hypertonic conditions, which induce vacuolar fission, lead to a rapid increase in PI(3,5)P$_2$ levels (Dove *et al.*, 1997; Bonangelino *et al.*, 2002; Duex *et al.*, 2006b). The rise in PI(3,5)P$_2$ triggers a release of Ca^{2+} through the exporter Yvc1 (Dong *et al.*, 2010). Deletion of either Fab1 or Yvc1 attenuates the ability of hypertonic conditions to cause membrane fission, indicating that the increase in PI(3,5)P$_2$ and subsequent release of Ca^{2+} are essential for membrane fission. PI(3,5)P$_2$ also binds directly to the vacuole-specific V-ATPase V$_O$ subunit Vph1 to trigger V-ATPase assembly (Li *et al.*, 2014). Vacuolar acidification itself has been shown to be an essential component of membrane fission, as inhibition of V-ATPase H$^+$ pumping activity leads to fission defects (Baars *et al.*, 2007). In this study we examined the ability of PI(3,5)P$_2$ to regulate membrane fusion.

RESULTS AND DISCUSSION
Dioctanoyl PI(3,5)P$_2$ inhibits vacuole homotypic fusion
Yeast vacuole fusion is promoted by a group of regulatory lipids including PI3P, PI4P, PI(4,5)P$_2$, ergosterol, and diacylglycerol, whereas vacuole fission during hyperosmotic shock is regulated by the PI(3,5)P$_2$ (Dove *et al.*, 1997; Bonangelino *et al.*, 2002; Duex *et al.*, 2006b). PI(3,5)P$_2$ is made sparingly and turned over rapidly, a likely indication that its prolonged presence or elevated concentration could have a negative impact on vacuole homeostasis. PI(3,5)P$_2$ is also

made under isotonic conditions, albeit at lower concentrations (Bonangelino *et al.*, 2002; Duex *et al.*, 2006b). Although much is known about PI(3,5)P$_2$, its effect during vacuole fusion is unclear. Here we tested the effects of adding exogenous dioctanoyl (C8) PI(3,5)P$_2$ to in vitro vacuole homotypic fusion reactions. We found that C8-PI(3,5)P$_2$ inhibited vacuole fusion in a dose-dependent manner with an IC$_{50}$ of ~100 μM (Figure 1A). The apparent IC$_{50}$ includes the large fraction of the lipid that does not incorporate into the membrane. Others have found that 340 μM C8-PI(4,5)P$_2$ is needed to reach 4 mol% incorporation into liposomes (Collins and Gordon, 2013). Thus, we can roughly estimate that 100 μM C8-PI(3,5)P$_2$ would translate to 1.2 mol% incorporated into vacuoles.

During hyperosmotic shock, PI(3,5)P$_2$ activates the TRP Ca^{2+} channel Yvc1. To test whether the inhibitory effect of PI(3,5)P$_2$ was due to Yvc1 activation, we used vacuoles from *yvc1Δ* yeast. The addition of C8-PI(3,5)P$_2$ to *yvc1Δ* vacuoles had an inhibitory effect on fusion nearly identical to that of WT vacuoles (Figure 1B). Thus, we can conclude that the effect of C8-PI(3,5)P$_2$ is independent of activating Yvc1 function. As a control we used the PI(3,5)P$_2$ precursor PI3P. WT vacuoles were treated with a curve of C8-PI3P and tested for fusion. Unlike the inhibitory effects of PI(3,5)P$_2$, there was no significant reduction in fusion with C8-PI3P (Figure 1C). To see whether the inhibitory effect of PI(3,5)P$_2$ was related to the presence of two phosphates on the head group, we used C8-PI(4,5)P$_2$ in fusion assays. We found that C8-PI(4,5)P$_2$ also inhibited vacuole fusion, albeit at a significantly higher concentration (IC$_{50}$ > 300 μM) relative to C8-PI(3,5)P$_2$ (Figure 1D). The difference in IC$_{50}$ values was likely due to nonoverlapping sets of interacting partners. For instance PI(4,5)P$_2$ interacts with twinfilin (Palmgren *et al.*, 2001), cofilin (Ojala *et al.*, 2001), and Spo14 (Sciorra *et al.*, 2002), while PI(3,5)P$_2$ interacts with Vph1 (Li *et al.*, 2014), Ivy1 (Malia *et al.*, 2018), Atg18 (Dove *et al.*, 2004), and Yvc1 (Dong *et al.*, 2010).

C8-PI(3,5)P$_2$ inhibits vacuole fusion at the docking stage
Previously, we found that adding C8-phosphatidic acid (PA) inhibited vacuole fusion at the priming stage by preventing the recruitment of Sec18 to *cis*-SNARE complexes (Starr *et al.*, 2016). To begin to determine at which stage PI(3,5)P$_2$ inhibited fusion, we first tested SNARE priming. When Sec18 is recruited to inactive SNAREs for priming, it associates with *cis*-SNARE complexes through its interactions with Sec17. Once Sec18 hydrolyzes ATP to dissociate SNAREs, Sec17 is released from the membrane (Mayer *et al.*, 1996). Thus, priming can be measured by the loss of Sec17 from the membrane. Here, fusion reactions were incubated with reaction buffer, C8-PI(3,5)P$_2$, or *N*-ethylmaleimide (NEM), a known inhibitor of priming (Paumet *et al.*, 2000). Individual reactions were incubated for specific times after which they were centrifuged to separate the membrane-bound (pellet) and solubilized (supernatant) fractions of Sec17. These experiments showed that PI(3,5)P$_2$ did not negatively affect SNARE priming, as levels of Sec17 were released similar to
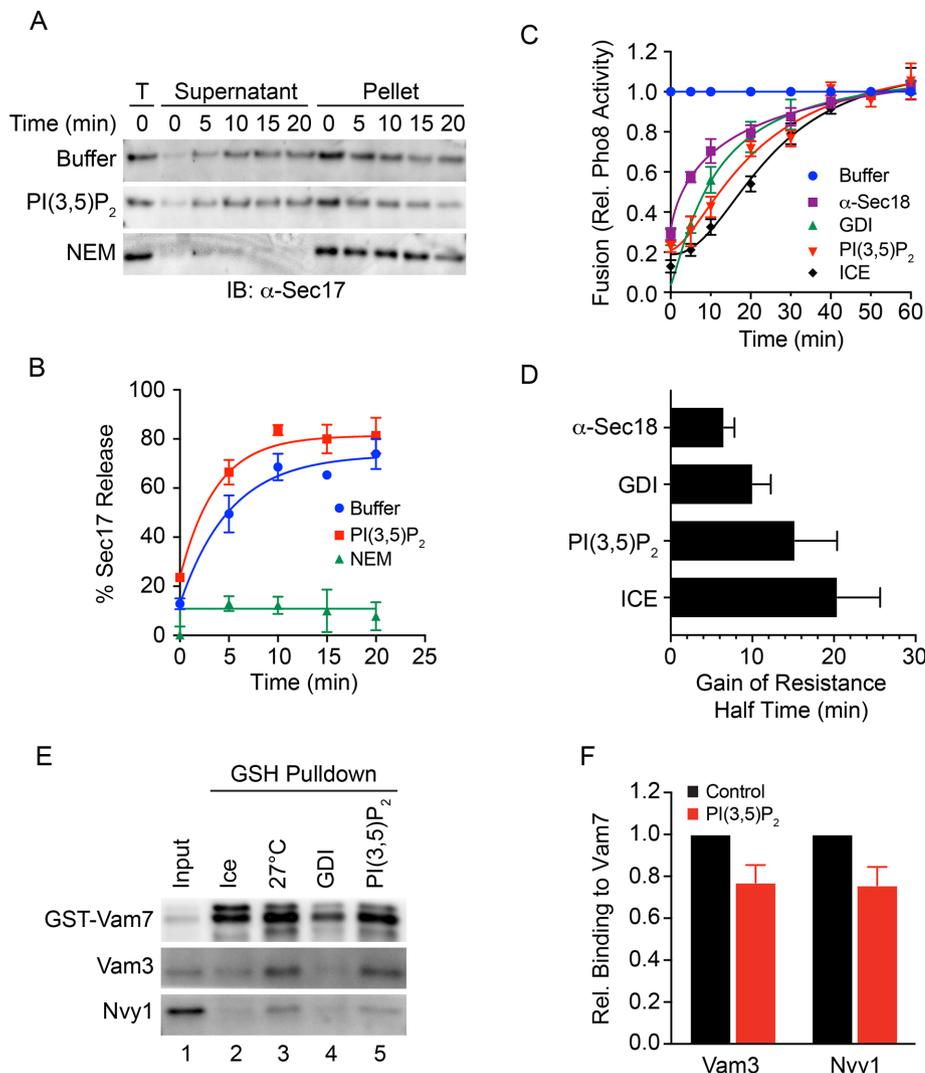
FIGURE 2: C8-PI(3,5)P$_2$ inhibits vacuole fusion at the docking stage. (A) WT vacuoles were monitored for Sec17 release of upon SNARE priming. Fusion reactions containing 3 μg of vacuoles were incubated with reaction buffer, 232 μM C8-PI(3,5)P$_2$, or 1 mM NEM. Vacuoles were incubated at 27°C for the indicated times, after which the organelles were pelleted by centrifugation. Released proteins in the supernatant were separated from the membrane-bound fraction. The membrane pellets were resuspended in volumes of buffer equal to the supernatant. Sec17 was detected by immunoblotting and the amount released was calculated by densitometry. (B) Normalized values were averaged and plotted over time of incubation. (C) Gain-of-resistance kinetic vacuole-fusion assays were performed in the presence of reaction buffer, 70 μg/ml anti-Sec18 IgG, 2 μM GDI, or C8-PI(3,5)P$_2$. Reactions were incubated at 27°C. Reactions were treated with reagents or shifted to ice at the indicated time points. Fusion inhibition was normalized to the reactions receiving buffer alone. (D) Calculated half-times of resistance from assays in C. (E) Vacuole fusion reactions were incubated with anti-Sec17 IgG to block SNARE priming. After incubation for 15 min at 27°C, select reactions were further treated with either reaction buffer, GDI, or C8-PI(3,5)P$_2$ and incubated for an additional 70 min. One reaction remained on ice for the duration of the assay. Reactions were then processed for glutathione pull down of GST–Vam7 protein complexes. Isolated protein complexes were immunoblotted for the presence of the SNAREs Vam3 and Nyv1. (F) Quantitation of SNARE complex formation in the presence or absence of C8-PI(3,5)P$_2$. Error bars are SEM ($n = 3$).

points throughout the incubation period. Fusion reactions become resistant to a reagent once the target of the inhibitor completes its function. Thus, inhibitors of early events (e.g., priming) would lose their effects before inhibitors of later stages (e.g., hemifusion). Through this approach, we found that PI(3,5)P$_2$ inhibited fusion late in the docking stage, as its resistance curve was after the anti-Sec18 immunoglobulin G (IgG) priming inhibition curve and the tethering inhibitor GDI (Figure 2, C and D). GDI extracts the Rab Ypt7 during fusion to prevent tethering and prevents the formation of *trans*-SNARE pairs (Haas *et al.*, 1995). The uninhibited control was normalized to 1 for each time point. These data indicate that PI(3,5)P$_2$ inhibits vacuole fusion after Ypt7-dependent vacuole association.

C8-PI(3,5)P$_2$ does not inhibit *trans*-SNARE complex formation

Owing to the indication that PI(3,5)P$_2$ inhibited vacuole fusion after tethering, we next examined whether SNARE complex formation occurred. For this, we used our GST–Vam7 bypass assay, where fusion reactions are blocked at the priming stage by anti-Sec17 IgG (Karunakaran and Fratti, 2013; Miner *et al.*, 2016). The added GST–Vam7 forms new *trans* complexes with free SNAREs (Merz and Wickner, 2004; Thorngren *et al.*, 2004). Between the addition of anti-Sec17 and Vam7, we further treated individual reactions with GDI or PI(3,5)P$_2$. Once GST–Vam7 was added, the reactions were incubated at 27°C or on ice as indicated. After incubation, the reactions were placed on ice and solubilized as described in *Materials and Methods*. GST–Vam7 SNARE complexes were isolated with reduced glutathione beads and SNARE complexes were detected by immunoblotting. Figure 2E shows that GST–Vam7 formed complexes with its cognate SNAREs Vam3 and Nyv1 when incubated at 27°C, whereas remaining on ice prevented complex formation. While GDI reduced SNARE complex formation, the addition of PI(3,5)P$_2$ had no effect on the interactions of these proteins. Quantitation of multiple experiments showed that PI(3,5)P$_2$ indeed had no significant effect on SNARE pair formation (Figure 2F).

Lipid mixing is blocked by C8-PI(3,5)P$_2$

Previous studies have shown that lysophosphatidylcholine (LPC) blocked fusion late in the pathway, with a gain-of-resistance curve similar to what we saw with PI(3,5)P$_2$ (Reese and Mayer, 2005). While LPC permitted SNARE complex assembly, it was shown that LPC blocked hemifusion (outer leaflet lipid mixing) in a dose-dependent manner. We next examined whether PI(3,5)P$_2$ had an effect similar to that of LPC in blocking outer leaflet lipid

those of the buffer control (Figure 2, A and B). In contrast, SNARE priming was inhibited by NEM, as shown by the complete blocking of Sec17 release.

To further resolve at which stage PI(3,5)P$_2$ inhibited fusion, we performed a temporal-gain-of-resistance assay (Sasser *et al.*, 2012a). Here, inhibitors were added to individual reactions at different time
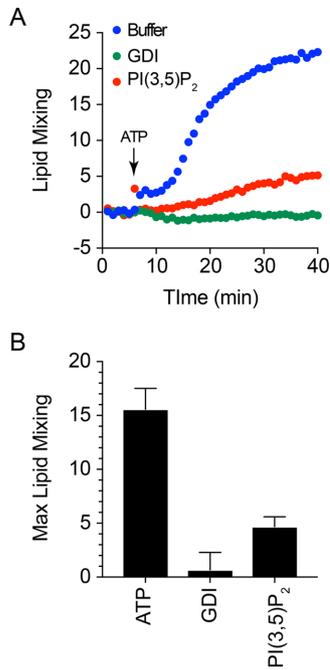
FIGURE 3: Lipid mixing is blocked by C8-PI(3,5)P$_2$. (A) Lipid-mixing assay measuring outer leaflet fusion, that is, hemifusion, were performed using vacuoles labeled with Rh-PE. Reactions were treated with either buffer, GDI, or C8-PI(3,5)P$_2$ and incubated for 40 min. Reactions were started by adding ATP after 5 min. Fluorescence was measured every 60 s and plotted against time as a percent of maximum fluorescence. (B) Quantitation of average maximum Rh-PE fluorescence. Error bars are SEM ($n = 3$).

mixing after allowing *trans*-SNARE complex formation. Lipid mixing was measured by the dequenching of Rhodamine-PE (Rh-PE) on the outer leaflets of vacuoles. Rh-PE–labeled vacuoles were incubated with an excess of unlabeled vacuoles. Upon the fusion of the outer leaflets, Rh-PE was diluted to restore fluorescence. Our results showed that PI(3,5)P$_2$ potently blocked lipid mixing, similarly to what was seen with LPC (Figure 3, A and B). As a negative control, we used GDI to block fusion at the tethering stage. These data indicate that PI(3,5)P$_2$ blocks fusion at a stage after *trans*-SNARE pairing but before lipid mixing can occur.

Fab1 mutants affect lipid mixing

To verify that an excess of PI(3,5)P$_2$ inhibits lipid mixing, we used vacuoles from yeast expressing the hyperactive kinase mutation *fab1^{T2250A}* (Lang *et al.*, 2017). As predicted, *fab1^{T2250A}* vacuoles failed to undergo lipid mixing (Figure 4, A and B). This was attributed to the increased production of PI(3,5)P$_2$ and is consistent with our data using exogenous lipid. This posed the question of whether lowering free PI(3,5)P$_2$ on *fab1^{T2250A}* vacuoles would restore lipid mixing. To this aim we used the PI(3,5)P$_2$ probe ML1-N, a polypeptide region at the N-terminus of the endolysosomal the TRPML Ca^{2+} channel (Dong *et al.*, 2010). We found that added 50 nM ML1-N partially restored lipid mixing (Figure 4J). This further supports the model in which an excess of free PI(3,5)P$_2$ negatively regulates vacuole fusion.

We next tested whether the lack of PI(3,5)P$_2$ would have the opposite effect on lipid mixing. To check this, we used vacuoles from yeast with the kinase dead mutant *fab1^{EEE}* (Li *et al.*, 2014). Although we expected to find elevated lipid mixing relative to WT vacuoles, we found that *fab1^{EEE}* vacuoles were blocked for lipid mixing (Figure 4, C and D). This suggests that some PI(3,5)P$_2$ production is needed for fusion, but an excess is inhibitory, which is consistent

with a biphasic role for the lipid in vacuole fusion. Biphasic roles for lipids are not unusual. For instance, PI(4,5)P$_2$ is needed for fusion, yet an excess of the lipid has an inhibitory effect. Another example lies in the turnover of PI(4,5)P$_2$ by phospholipase C (Plc1) to make diacylglycerol. It was shown that while low levels of Plc1 enhanced fusion, excess Plc1 blocked fusion altogether (Jun *et al.*, 2004).

Finally, we used *fig4Δ* vacuoles, which produce reduced amounts of PI(3,5)P$_2$ in comparison with WT cells. We found that *fig4Δ* vacuoles showed a modest reduction in lipid mixing (Figure 4, E and F). This suggests that the reduced PI(3,5)P$_2$ levels associated with *fig4Δ* cells are sufficient to support lipid mixing, albeit at reduced efficiency. Together, these data suggest that the transition from docking to the hemifusion stage requires some Fab1 activity, but augmented PI(3,5)P$_2$ production is inhibitory.

To further test the effects of modulating PI(3,5)P$_2$ concentrations on lipid mixing, we asked whether adding C8-PI(3,5)P$_2$ to *fab1^{EEE}* or *fig4Δ* vacuoles would restore lipid mixing. When *fig4Δ* vacuoles were treated with 25, 50, or 100 µM C8-PI(3,5)P$_2$ we found that lipid mixing was inhibited. However, when they were compared with WT, we discovered that the inhibitory power of C8-PI(3,5)P$_2$ was not as potent with *fig4Δ* vacuoles (Figure 4G). Comparison of the changes in lipid mixing due to 100 µM C8-PI(3,5)P$_2$ showed an ~50% reduction in lipid mixing inhibition of *fig4Δ* vacuoles (Figure 4H). This was not due to complete blocking of lipid mixing, as it can be further inhibited at higher C8-PI(3,5)P$_2$ concentrations (Figure 3). We attribute the reduced inhibition of *fig4Δ* vacuole lipid mixing to the reduced endogenous levels of PI(3,5)P2 associated with the deletion. Thus, the combined amount of endogenous and C8-PI(3,5)P$_2$ in *fig4Δ* vacuoles was less than ino WT vacuoles, resulting in different effects. This also shows that sufficient endogenous PI(3,5)P$_2$ is present on isolated vacuoles to affect fusion efficiency.

In parallel, we found that adding C8-PI(3,5)P$_2$ had no effect on *fab1^{EEE}* lipid mixing (Figure 4J). The lack of any rescue suggested that other factors could be affected by the lack of Fab1 activity. Western blotting of known fusion factors on isolated vacuoles showed that Sec17 and Mon1 were reduced on both *fab1^{EEE}* and *fab1^{T2250A}* vacuoles (Figure 4K). Sec17 is needed for SNARE priming (Mayer *et al.*, 1996), while Mon1 is the guanine nucleotide exchange factor or the Rab Ypt7 (Nordmann *et al.*, 2010). In addition, *fab1^{EEE}* vacuoles contained reduced levels of Ycf1, an ABC transporter needed for efficient vacuole fusion (Sasser *et al.*, 2013). A reduction in any of these factors could be expected to affect lipid mixing negatively. Other key factors such as SNAREs, HOPS, or Ypt7 were not altered on these vacuoles, and the normal amount of Ypt7 suggested that sufficient Mon1 was present to recruit the Rab. It should be noted that these blots were not comprehensive and there could be further changes in protein sorting in *fab1^{EEE}* and *fab1^{T2250A}* that could alter vacuole homeostasis.

Endogenous PI(3,5)P$_2$ on isolated vacuoles and fusion

Thus far, our studies show that while high levels of PI(3,5)P$_2$ potently inhibit fusion, lower concentrations are in fact beneficial for fusion. To further investigate this, we used the PI(3,5)P$_2$ ligand ML1-N described above. We added a curve of purified GST-ML1-N to fusion reactions and found that fusion was completely blocked (Figure 5A). This suggests that the endogenous vacuolar PI(3,5)P$_2$ plays a positive role in the fusion pathway.

To visualize endogenous levels of vacuolar PI(3,5)P$_2$, we used Cy3-labeled GST-ML1-N to perform docking experiments. Here we used WT, *fab1^{EEE}*, and *fab1^{T2250A}* vacuoles. Cy3-ML1-N was added to vacuoles incubated for 20 min at 27°C to allow docking. After incubation, vacuoles were stained with MDY-64 and examined by
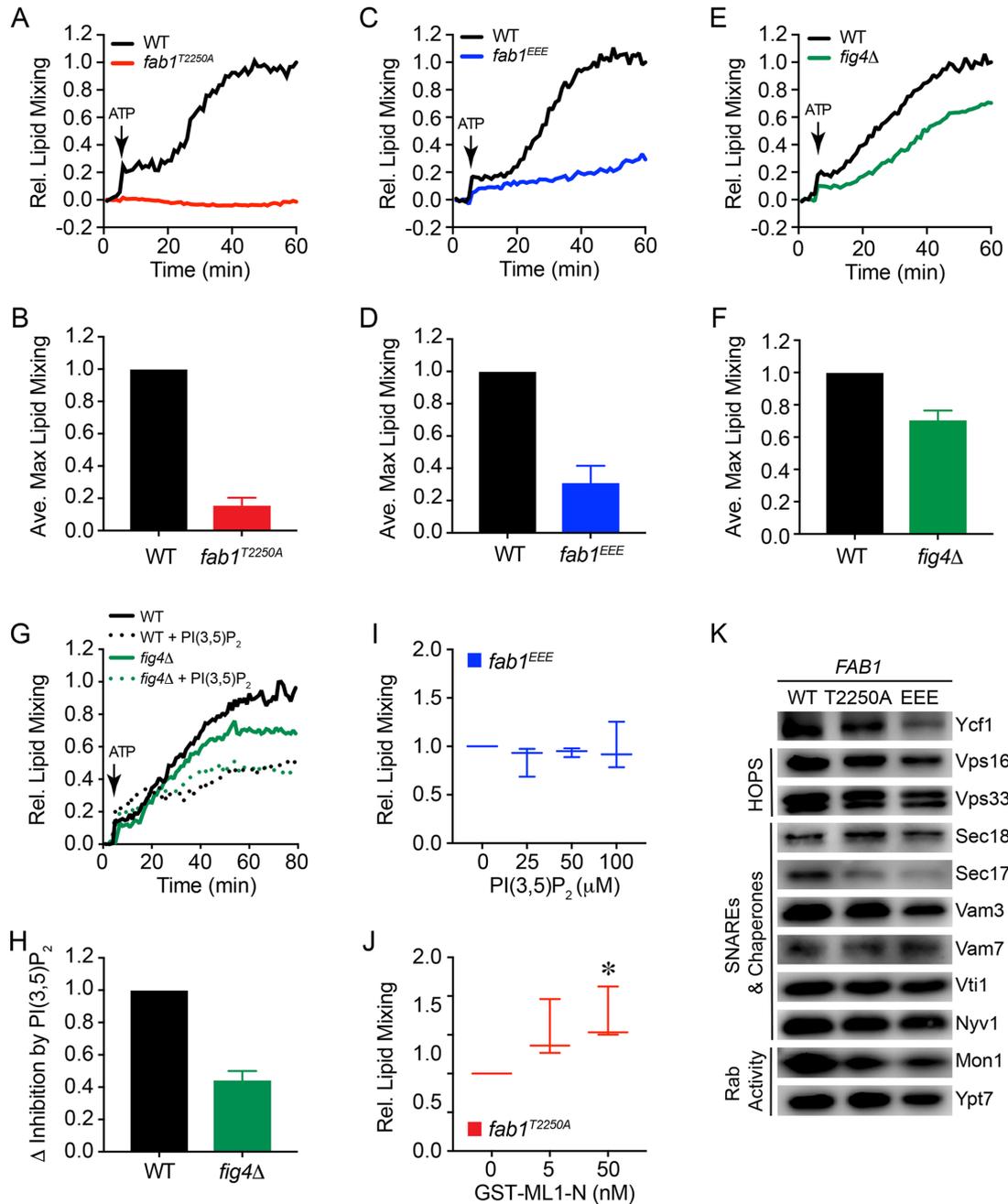
FIGURE 4: Fab1 mutants block lipid mixing. Lipid-mixing assays were performed with WT, $fab1^{T2250A}$ (A, B), $fab1^{EEE}$ (C, D), or $fig4\Delta$ (E, F) vacuoles. Reactions were started with the addition of ATP after 5 min and incubated for 60 min. Fluorescence was measured every 60 s. B, D, and F show quantitation of average maximum Rh-PE fluorescence. (G) WT and $fig4\Delta$ vacuoles were treated with C8-PI(3,5)P_2 and tested for lipid mixing. (H) Comparison of the inhibitory effects of C8-PI(3,5)P_2 on lipid mixing. The inhibition of WT vacuole lipid mixing by C8-PI(3,5)P_2 was normalized to 1 and compared with the relative inhibition of $fig4\Delta$ vacuole lipid mixing. (I) $fab1^{EEE}$ vacuoles were treated with C8-PI(3,5)P_2 and tested for lipid mixing. The amount of lipid mixing at the end of 60 min in the absence of C8-PI(3,5)P_2 was normalized to 1 and compared with the relative results in the presence of C8-PI(3,5)P_2 at the indicated concentrations. Data are represented as whisker plots. (J) $fab1^{T2250A}$ vacuoles were treated with ML1-N and tested for lipid mixing. The terminal level of lipid mixing in the untreated sample was normalized to 1 and compared with the relative results in the presence of ML1-N. (K) Analysis of fusion factors on purified vacuoles (5 µg protein) from WT, $fab1^{EEE}$, or $fab1^{T2250A}$ yeast. Antibodies against the indicated proteins were used for immunoblotting. Error bars are SEM ($n = 3$). *$p < 0.5$.

fluorescence microscopy. Equal exposure times were used for each strain. Z-stacks of images were taken for ten fields per strain and deconvolved using Zeiss Axiovision software. Figure 5B shows equatorial images of docked vacuoles. WT vacuoles were stained with Cy3-ML1, which clustered at the junctions where vacuoles come into contact, similarly to the localization of other regulatory lipids as previously shown (Fratti *et al.*, 2004). $Fab1^{EEE}$ vacuoles showed no staining whatsoever, in keeping with the lack of kinase activity. This also illustrates the specificity of Cy3-ML1 for PI(3,5)P_2, as other PIs such as PI3P and PI(4,5)P_2 are present in the absence of

A

IC_{50} = 540 nM

B
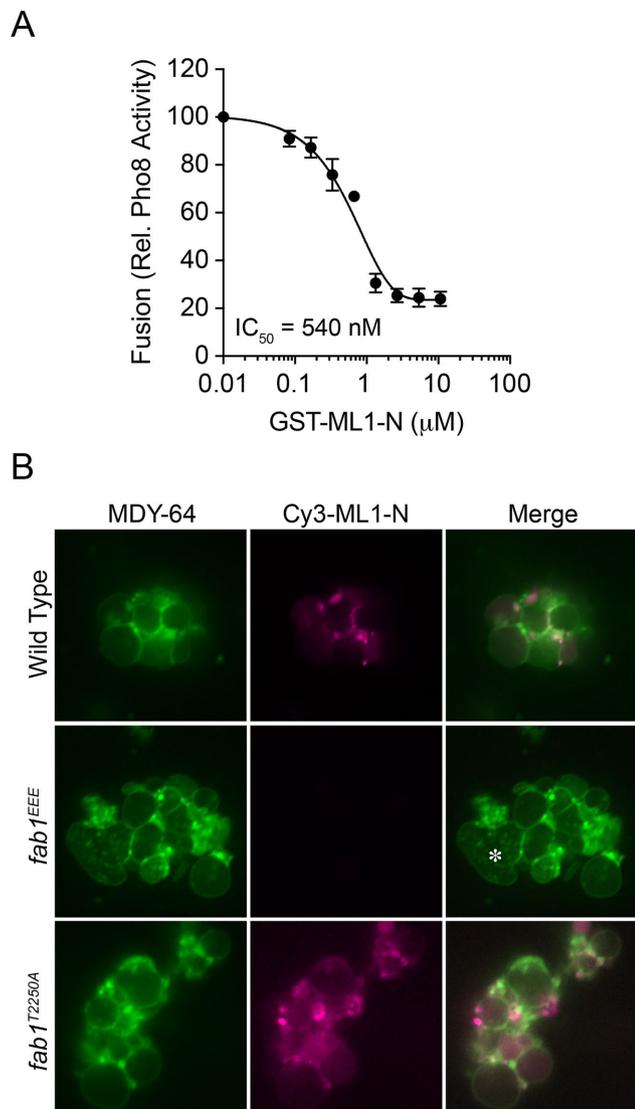
FIGURE 5: Endogenous PI(3,5)P_2 on isolated vacuoles. (A) WT vacuoles were incubated with ML1-N to bind PI(3,5)P_2. (B) Docking reactions of vacuoles incubated with Cy3-ML1-N. Vacuoles were counterstained with the MDY-64 to label the entirety of the membranes. Representative vacuole clusters are shown for qualitative assessment of PI(3,5)P_2 distribution.

Fab1 activity (Gary *et al.*, 1998). It is also important to note that *fab1^EEE* vacuoles were commonly enlarged and deformed, as exemplified by the selected cluster (asterisk). This is in agreement with the enlarged vacuoles seen in *fab1Δ* cells. Finally, we observed increased Cy3-ML1 staining on *fab1^T2250A* vacuoles, as expected in the presence of elevated PI(3,5)P_2. Interestingly, we also observed an increase in small vesicles with increased Cy3-ML1-N staining tightly apposed to larger vacuoles. Although further detailed testing would be required to verify it, these small vesicles could be the result of vacuole fission linked to the hyperactive nature of this mutant.

Taken together, the results of this study have demonstrated that while PI(3,5)P_2 is needed for vacuole fusion, an excess of the lipid strongly blocks the system. This leaves us with the question of how PI(3,5)P_2 directly affects fusion. One possible mechanism for the inhibition of fusion could be linked to the vacuolar ATPase. Others have reported that PI(3,5)P_2 stabilizes the interactions of the V_1 and V_O components of the V-ATPase (Li *et al.*, 2014). This occurs through

the direct interactions of the V_O subunit Vph1 and PI(3,5)P_2, which promote binding of the V_1 complex. The increased assembly of the V_1–V_O holoenzyme would in turn deplete free V_O complexes on the vacuole membrane. The significance of altering the levels of free V_O complexes and vacuole fusion lies in the ability of V_O complexes to interact in *trans* between apposed membranes. Mayer and colleagues originally found that the formation of *trans* V_O–V_O complexes plays a role in membrane fusion (Peters *et al.*, 2001). Since their discovery, several other groups using various systems found that V_O plays important noncanonical roles in membrane fusion, including the release of insulin (Sun-Wada *et al.*, 2006), phagosome–lysosome fusion (Peri and Nusslein-Volhard, 2008), and the release of exosomes through the fusion of multivesicular bodies with the plasma membrane (Liégeois *et al.*, 2006). The c-rings of the V_O also interact in *trans* between membranes to form conductance channels through their proteolipid pores (Couoh-Cardel *et al.*, 2016). Although PI(3,5)P_2 has not been shown to reduce V_O–V_O *trans* complexes directly, it stands to reason that the increase in V_1–V_O complexes would in turn diminish the former and potentially alter fusion efficiency.

Another potential target for PI(3,5)P_2 could involve altering Ca^{2+} transport across the vacuole membrane. During salt shock, PI(3,5)P_2 is rapidly synthesized and interacts with the TRP channel Yvc1 to release vacuolar Ca^{2+} stores. Because vacuolar Ca^{2+} stores are also released in response to the formation of *trans*-SNARE pairs (Merz and Wickner, 2004), we initially hypothesized that PI(3,5)P_2 could affect fusion through interactions with Yvc1. However, vacuoles from *yvc1Δ* yeast were equally susceptible to PI(3,5)P_2 relative to the WT parents, suggesting that PI(3,5)P_2 has a different target for the inhibition of fusion. Taken together with the studies on PI(3,5)P_2 and vacuole fission, we propose that this lipid performs two opposing functions as a molecular switch to go between fission and fusion.

MATERIALS AND METHODS
Reagents
Soluble reagents were dissolved in PIPES–sorbitol (PS) buffer (20 mM PIPES-KOH, pH 6.8, 200 mM sorbitol) with 125 mM KCl unless indicated otherwise. Anti-Sec17 IgG, anti-Sec18 and Pbi2 (Protease B inhibitor) were prepared as described previously (Haas and Wickner, 1996; Mayer *et al.*, 1996; Slusarewicz *et al.*, 1997). C8-PI3P (1,2-dioctanoyl-phosphatidylinositol 3-phosphate) and C8-PI(4,5)P_2 (1,2-dioctanoyl-phosphatidylinositol 3,5-bisphosphate) were purchased from Echelon. Recombinant GST–Vam7 and GDI were prepared as previously described (Fratti *et al.*, 2007; Fratti and Wickner, 2007; Starai *et al.*, 2007). Plasmid to produce recombinant GST-ML1-N was a gift from H. Xu (University of Michigan). GST-ML1-N was prepared as described and dialyzed against PS buffer with 125 mM KCl (Dong *et al.*, 2010). Lissamine Rhodamine (Rh-PE) was from ThermoFisher. NEM (N-ethylmaleimide) was from Sigma.

Strains
BJ3505 (Jones *et al.*, 1982) and DKY6281 (Haas *et al.*, 1994) were used for fusion assays (Table S1 in the Supplemental Material). *YVC1* was deleted by homologous recombination using PCR products amplified from pFA6-KanMX6 with the primers 5′-YVC1-KO and 3′-YVC1-KO with homology flanking the *YVC1* coding sequence (Table S2 in the Supplemental Material). The PCR product was transformed into BJ3505 and DKY6281 yeast by standard lithium acetate methods and plated on YPD media containing G418 (250 μg/ml) to generate BJ3505 *yvc1Δ::kanMX6* (RFY74) and DKY6281 *yvc1Δ::kanMX6* (RFY75). Similarly, *FAB1* was deleted by recombination using the primers 5′-FAB1-KO and 3′-FAB1-KO to

generate BJ3505 *fab1Δ::kanMX6* (RFY76). RFY76 was transformed with a plasmid encoding the hyperactive kinase mutant *fab1^{T2250A}* (pRS416-FAB1-T2250A) and grown in selective media lacking uracil to make RFY78 (Lang *et al.*, 2017). Similarly, a plasmid encoding the kinase–dead mutant *fab1^{EEE}* (pRS416-FAB1-EEE) was transformed into RFY76 to make RFY80 (Li *et al.*, 2014). Plasmids harboring Fab1 mutants were a gift from Lois Weisman (University of Michigan). *FIG4* was deleted through recombination as described above, using PCR products amplified from pAG32 with the primers 5′-FIG4-KO and 3′-FIG4-KO to generate BJ3505 *fig4Δ::hphMX4* (RFY82). Transformants were grown in YPD with hygromycin (250 µg/ml).

Vacuole isolation and in vitro fusion assay

Vacuoles were isolated as described (Haas *et al.*, 1994). In vitro fusion reactions (30 µl) contained 3 µg each of vacuoles from BJ3505 (*PHO8 pep4Δ*) and DKY6281 (*pho8Δ PEP4*) backgrounds, reaction buffer (20 mM PIPES-KOH, pH 6.8, 200 mM sorbitol, 125 mM KCl, 5 mM MgCl$_2$), ATP regenerating system (1 mM ATP, 0.1 mg/ml creatine kinase, 29 mM creatine phosphate), 10 µM CoA, and 283 nM Pbi2. Fusion was determined by the processing of pro-Pho8 (alkaline phosphatase) from BJ3505 by the Pep4 protease from DK6281. Fusion reactions were incubated at 27°C for 90 min and Pho8 activity was measured in 250 mM Tris-HCl, pH 8.5, 0.4% Triton X-100, 10 mM MgCl$_2$, and 1 mM *p*-nitrophenyl phosphate. Pho8 activity was stopped after 5 min by addition of 1 M glycine, pH 11, and fusion units were measured by determining the *p*-nitrophenolate produced by detecting absorbance at 400 nm.

GST–Vam7 SNARE complex isolation

SNARE complex isolation was performed as described previously using GST–Vam7 (Fratti *et al.*, 2007; Fratti and Wickner, 2007; Miner *et al.*, 2016, 2017). Briefly, 5× fusion reactions were incubated with 85 µg/ml anti-Sec17 IgG to block priming. After 15 min, 2 µM GDI or 232 µM C8-PI(3,5)P$_2$ was added to selected reactions and incubated for an additional 5 min before the addition of 150 nM GST–Vam7. After a total of 90 min, reactions were sedimented (11,000 × *g*, 10 min, 4°C), and the supernatants were discarded before the extraction of vacuoles with solubilization buffer (SB: 20 mM HEPES-KOH, pH 7.4, 100 mM NaCl, 2 mM EDTA, 20% glycerol, 0.5% Triton X-100, 1 mM dithiothreitol) with protease inhibitors (1 mM PMSF, 10 µM Pefabloc-SC, 5 µM pepstatin A, and 1 µM leupeptin). Vacuole pellets were overlaid with 100 µl SB and resuspended gently. An additional 100 µl SB was added, gently mixed, and incubated on ice for 20 min. Insoluble debris was sedimented (16,000 × *g*, 10 min, 4°C) and 176 µl of supernatants was removed and placed in chilled tubes. Next, 16 µl was removed from each reaction as 10% total samples, mixed with 8 µl of 3X SDS loading buffer, and heated (95°C, 5 min). Equilibrated glutathione beads (30 µl) were incubated with the remaining extracts (15 h, 4°C, nutation). Beads were sedimented and washed 5× with 1 ml SB (735 × *g*, 2 min, 4°C), and bound material was eluted with 40 µl 1× SDS loading buffer. Protein complexes were examined by Western blotting.

Lipid mixing

Lipid mixing assays were conducted using rhodamine B DHPE (Rh-PE; Thermo-Fisher) as described (Sasser *et al.*, 2012a,b, 2013; Miner *et al.*, 2016, 2017; Karunakaran and Fratti, 2013). BJ3505 vacuoles (300 µg) were isolated and then incubated in 400 µl of PS buffer containing 150 µM Rh-PE (10 min, 4°C, nutating). Next, 800 µl of 15% Ficoll was added and then transferred to an 11 × 60 mm ultracentrifuge tube, overlaid with 1.2 ml of 8 and 4% and 0.5 ml of PS

buffer. Labeled vacuoles were isolated by centrifugation (105,200 × *g*, 25 min, 4°C, SW-60 Ti rotor) and recovered from the 0–4% Ficoll interface. Lipid mixing assays (90 µl) contained 2 µg of labeled vacuoles and 16 µg of unlabeled vacuoles in fusion buffer. Reaction mixtures were transferred to a black, half-volume 96-well flat-bottom microtiter plate (Corning 3686) on ice. The plate was transferred to a fluorescence plate reader at 27°C to start the reactions. Measurements were taken every 60 s for 40 min, yielding fluorescence values (λ_{ex} = 544 nm; λ_{em} = 590 nm) at the onset (F_0) and during the reaction (F_t). After 40 min, 0.45% (vol/vol) Triton X-100 was added and the final 10 measurements were averaged to give the value of fluorescence after infinite dilution (F_{TX100}). The relative fluorescence change $\Delta F_t/F_{TX100} = (F_t - F_0)/F_{TX100} - F_0$ was calculated.

Vacuole docking

Docking reactions (30 µl) containing 6 µg of vacuoles from WT, *fab1^{EEE}*, *fab1^{T2250A}*, or *fig4Δ* yeast were incubated in docking buffer (20 mM PIPES-KOH, pH 6.8, 200 mM sorbitol, 100 mM KCl, 0.5 mM MgCl$_2$), ATP regenerating system (0.3 mM ATP, 0.7 mg/ml creatine kinase, 6 mM creatine phosphate), 20 µM CoA, and 283 nM Pbi2 (Fratti *et al.*, 2004). PI(3,5)P$_2$ was labeled with 2.5 µM Cy3-GST-ML1-N. Reactions were incubated at 27°C for 20 min. After incubation, reaction tubes were placed on ice and vacuoles were stained with 1 µM MDY-64. Reactions were next mixed with 50 µl of 0.6% low-melt agarose (in PS buffer), vortexed to disrupt nonspecific clustering, and mounted on slides for observation by fluorescence microscopy. Images were acquired using a Zeiss Axio Observer Z1 inverted microscope equipped with an X-Cite 120XL light source, a Plan Apochromat 63X oil objective (NA 1.4), and an AxioCam CCD camera.

REFERENCES

Andersen OS, Koeppe RE 2nd (2007). Bilayer thickness and membrane protein function: an energetic perspective. Annu Rev Biophys Biomol Struct 36, 107–130.

Baars TL, Petri S, Peters C, Mayer A (2007). Role of the V-ATPase in regulation of the vacuolar fission-fusion equilibrium. Mol Biol Cell 18, 3873–3882.

Boeddinghaus C, Merz AJ, Laage R, Ungermann C (2002). A cycle of Vam7p release from and PtdIns 3-P-dependent rebinding to the yeast vacuole is required for homotypic vacuole fusion. J Cell Biol 157, 79–89.

Bonangelino CJ, Nau JJ, Duex JE, Brinkman M, Wurmser AE, Gary JD, Emr SD, Weisman LS (2002). Osmotic stress-induced increase of phosphatidylinositol 3,5-bisphosphate requires Vac14p, an activator of the lipid kinase Fab1p. J Cell Biol 156, 1015–1028.

Botelho RJ, Efe JA, Teis D, Emr SD (2008). Assembly of a Fab1 phosphoinositide kinase signaling complex requires the Fig4 phosphoinositide phosphatase. Mol Biol Cell 19, 4273–4286.

Carman GM, Han GS (2009). Regulation of phospholipid synthesis in yeast. J Lipid Res 50(Suppl), S69–S73.

Collins MD, Gordon SE (2013). Short-chain phosphoinositide partitioning into plasma membrane models. Biophys J 105, 2485–2494.

Couoh-Cardel S, Hsueh YC, Wilkens S, Movileanu L (2016). Yeast V-ATPase proteolipid ring acts as a large-conductance transmembrane protein pore. Sci Rep 6, 24774.

Dong XP, Shen D, Wang X, Dawson T, Li X, Zhang Q, Cheng X, Zhang Y, Weisman LS, Delling M, Xu H (2010). PI(3,5)P2 controls membrane trafficking by direct activation of mucolipin Ca(2+) release channels in the endolysosome. Nat Commun 1, 38.

Dove SK, Cooke FT, Douglas MR, Sayers LG, Parker PJ, Michell RH (1997). Osmotic stress activates phosphatidylinositol-3,5-bisphosphate synthesis. Nature 390, 187–192.

Dove SK, Piper RC, McEwen RK, Yu JW, King MC, Hughes DC, Thuring J, Holmes AB, Cooke FT, Michell RH, *et al.* (2004). Svp1p defines a family of phosphatidylinositol 3,5-bisphosphate effectors. EMBO J 23, 1922–1933.

Duex JE, Nau JJ, Kauffman EJ, Weisman LS (2006a). Phosphoinositide 5-phosphatase Fig 4p is required for both acute rise and subsequent fall in stress-induced phosphatidylinositol 3,5-bisphosphate levels. Eukaryot Cell 5, 723–731.

Duex JE, Tang F, Weisman LS (2006b). The Vac14p-Fig4p complex acts independently of Vac7p and couples PI3,5P2 synthesis and turnover. J Cell Biol 172, 693–704.

Efe JA, Botelho RJ, Emr SD (2007). Atg18 regulates organelle morphology and Fab1 kinase activity independent of its membrane recruitment by phosphatidylinositol 3,5-bisphosphate. Mol Biol Cell 18, 4232–4244.

Fratti RA, Collins KM, Hickey CM, Wickner W (2007). Stringent 3Q: 1R composition of the SNARE 0-layer can be bypassed for fusion by compensatory SNARE mutation or by lipid bilayer modification. J Biol Chem 282, 14861–14867.

Fratti RA, Jun Y, Merz AJ, Margolis N, Wickner W (2004). Interdependent assembly of specific regulatory lipids and membrane fusion proteins into the vertex ring domain of docked vacuoles. J Cell Biol 167, 1087–1098.

Fratti RA, Wickner W (2007). Distinct targeting and fusion functions of the PX and SNARE domains of yeast vacuolar Vam7p. J Biol Chem 282, 13133–13138.

Gary JD, Sato TK, Stefan CJ, Bonangelino CJ, Weisman LS, Emr SD (2002). Regulation of fab1 phosphatidylinositol 3-phosphate 5-kinase pathway by vac7 protein and fig4, a polyphosphoinositide phosphatase family member. Mol Biol Cell 13, 1238–1251.

Gary JD, Wurmser AE, Bonangelino CJ, Weisman LS, Emr SD (1998). Fab1p is essential for PtdIns(3)P 5-kinase activity and the maintenance of vacuolar size and membrane homeostasis. J Cell Biol 143, 65–79.

Haas A, Conradt B, Wickner W (1994). G-protein ligands inhibit in vitro reactions of vacuole inheritance. J Cell Biol 126, 87–97.

Haas A, Scheglmann D, Lazar T, Gallwitz D, Wickner W (1995). The GTPase Ypt7p of *Saccharomyces cerevisiae* is required on both partner vacuoles for the homotypic fusion step of vacuole inheritance. EMBO J 14, 5258–5270.

Haas A, Wickner W (1996). Homotypic vacuole fusion requires Sec17p (yeast alpha-SNAP) and Sec18p (yeast NSF). EMBO J 15, 3296–3305.

Jin N, Chow CY, Liu L, Zolov SN, Bronson R, Davisson M, Petersen JL, Zhang Y, Park S, Duex JE, *et al.* (2008). VAC14 nucleates a protein complex essential for the acute interconversion of PI3P and PI(3,5)P(2) in yeast and mouse. EMBO J 27, 3221–3234.

Jones EW, Zubenko GS, Parker RR (1982). PEP4 gene function is required for expression of several vacuolar hydrolases in *Saccharomyces cerevisiae*. Genetics 102, 665–677.

Jun Y, Fratti RA, Wickner W (2004). Diacylglycerol and its formation by phospholipase C regulate Rab- and SNARE-dependent yeast vacuole fusion. J Biol Chem 279, 53186–53195.

Karunakaran S, Fratti R (2013). The lipid composition and physical properties of the yeast vacuole affect the hemifusion–fusion transition. Traffic 14, 650–662.

Kiontke S, Langemeyer L, Kuhlee A, Schuback S, Raunser S, Ungermann C, Kümmel D (2017). Architecture and mechanism of the late endosomal Rab7-like Ypt7 guanine nucleotide exchange factor complex Mon1-Ccz1. Nat Commun 8, 14034.

Lang MJ, Strunk BS, Azad N, Petersen JL, Weisman LS (2017). An intramolecular interaction within the lipid kinase Fab1 regulates cellular phosphatidylinositol 3,5-bisphosphate lipid levels. Mol Biol Cell 28, 858–864.

Lawrence G, Brown CC, Flood BA, Karunakaran S, Cabrera M, Nordmann M, Ungermann C, Fratti RA (2014). Dynamic association of the PI3P-interacting Mon1-Ccz1 GEF with vacuoles is controlled through its phosphorylation by the type-1 casein kinase Yck3. Mol Biol Cell 25, 1608–1619.

Li SC, Diakov TT, Xu T, Tarsio M, Zhu W, Couoh-Cardel S, Weisman LS, Kane PM (2014). The signaling lipid PI(3,5)P$_2$ stabilizes V$_1$-V(o) sector interactions and activates the V-ATPase. Mol Biol Cell 25, 1251–1262.

Liégeois S, Benedetto A, Garnier JM, Schwab Y, Labouesse M (2006). The V0-ATPase mediates apical secretion of exosomes containing Hedgehog-related proteins in *Caenorhabditis elegans*. J Cell Biol 173, 949–961.

Malia PC, Numrich J, Nishimura T, González Montoro A, Stefan CJ, Ungermann C (2018). Control of vacuole membrane homeostasis by a resident PI-3,5-kinase inhibitor. Proc Natl Acad Sci USA 115, 4684–4689.

Mayer A, Wickner W, Haas A (1996). Sec18p (NSF)-driven release of Sec17p (alpha-SNAP) can precede docking and fusion of yeast vacuoles. Cell 85, 83–94.

Merz AJ, Wickner W (2004). *Trans*-SNARE interactions elicit Ca2+ efflux from the yeast vacuole lumen. J Cell Biol 164, 195–206.

Miner GE, Starr ML, Hurst LR, Fratti RA (2017). Deleting the DAG kinase Dgk1 augments yeast vacuole fusion through increased Ypt7 activity and altered membrane fluidity. Traffic 18, 315–329.

Miner GE, Starr ML, Hurst LR, Sparks RP, Padolina M, Fratti RA (2016). The central polybasic region of the soluble SNARE (soluble N-ethyl-maleimide-sensitive factor attachment protein receptor) Vam7 affects binding to phosphatidylinositol 3-phosphate by the PX (Phox homology) domain. J Biol Chem 291, 17651–17663.

Nordmann M, Cabrera M, Perz A, Brocker C, Ostrowicz C, Engelbrecht-Vandre S, Ungermann C (2010). The Mon1–Ccz1 complex is the GEF of the late endosomal Rab7 homolog Ypt7. Curr Biol 20, 1654–1659.

Ojala PJ, Paavilainen V, Lappalainen P (2001). Identification of yeast cofilin residues specific for actin monomer and PIP2 binding. Biochemistry 40, 15562–15569.

Palmgren S, Ojala PJ, Wear MA, Cooper JA, Lappalainen P (2001). Interactions with PIP2, ADP-actin monomers, and capping protein regulate the activity and localization of yeast twinfilin. J Cell Biol 155, 251–260.

Paumet F, Le Mao J, Martin S, Galli T, David B, Blank U, Roa M (2000). Soluble NSF attachment protein receptors (SNAREs) in RBL-2H3 mast cells: functional role of syntaxin 4 in exocytosis and identification of a vesicle-associated membrane protein 8-containing secretory compartment. J Immunol 164, 5850–5857.

Peri F, Nusslein-Volhard C (2008). Live imaging of neuronal degradation by microglia reveals a role for v0-ATPase a1 in phagosomal fusion in vivo. Cell 133, 916–927.

Peters C, Bayer MJ, Buhler S, Andersen JS, Mann M, Mayer A (2001). Trans-complex formation by proteolipid channels in the terminal phase of membrane fusion. Nature 409, 581–588.

Reese C, Mayer A (2005). Transition from hemifusion to pore opening is rate limiting for vacuole membrane fusion. J Cell Biol 171, 981–990.

Sasser T, Qiu QS, Karunakaran S, Padolina M, Reyes A, Flood B, Smith S, Gonzales C, Fratti RA (2012a). Yeast lipin 1 orthologue pah1p regulates vacuole homeostasis and membrane fusion. J Biol Chem 287, 2221–2236.

Sasser TL, Lawrence G, Karunakaran S, Brown C, Fratti RA (2013). The yeast ABC transporter Ycf1p enhances the recruitment of the soluble SNARE Vam7p to vacuoles for efficient membrane fusion. J Biol Chem 288, 18300–18310.

Sasser TL, Padolina M, Fratti RA (2012b). The yeast vacuolar ABC transporter Ybt1p regulates membrane fusion through Ca2+ transport modulation. Biochem J 448, 365–372.

Sbrissa D, Ikonomov OC, Fu Z, Ijuin T, Gruenberg J, Takenawa T, Shisheva A (2007). Core protein machinery for mammalian phosphatidylinositol 3,5-bisphosphate synthesis and turnover that regulates the progression of endosomal transport. Novel Sac phosphatase joins the ArPIKfyve-PIKfyve complex. J Biol Chem 282, 23878–23891.

Sciorra VA, Rudge SA, Wang J, McLaughlin S, Engebrecht J, Morris AJ (2002). Dual role for phosphoinositides in regulation of yeast and mammalian phospholipase D enzymes. J Cell Biol 159, 1039–1049.

Simons K, Toomre D (2000). Lipid rafts and signal transduction. Nat Rev Mol Cell Biol 1, 31–39.

Slusarewicz P, Xu Z, Seefeld K, Haas A, Wickner WT (1997). I2B is a small cytosolic protein that participates in vacuole fusion. Proc Natl Acad Sci USA 94, 5582–5587.

Starai VJ, Jun Y, Wickner W (2007). Excess vacuolar SNAREs drive lysis and Rab bypass fusion. Proc Natl Acad Sci USA 104, 13551–13558.

Starr ML, Hurst LR, Fratti RA (2016). Phosphatidic acid sequesters Sec18p from cis-SNARE complexes to inhibit priming. Traffic 17, 1091–1109.

Sun-Wada GH, Toyomura T, Murata Y, Yamamoto A, Futai M, Wada Y (2006). The a3 isoform of V-ATPase regulates insulin secretion from pancreatic beta-cells. J Cell Sci 119, 4531–4540.

Thorngren N, Collins KM, Fratti RA, Wickner W, Merz AJ (2004). A soluble SNARE drives rapid docking, bypassing ATP and Sec17/18p for vacuole fusion. EMBO J 23, 2765–2776.

Yamamoto A, DeWald DB, Boronenkov IV, Anderson RA, Emr SD, Koshland D (1995). Novel PI(4)P 5-kinase homologue, Fab1p, essential for normal vacuole function and morphology in yeast. Mol Biol Cell 6, 525–539.

Zick M, Stroupe C, Orr A, Douville D, Wickner WT (2014). Membranes linked by trans-SNARE complexes require lipids prone to non-bilayer structure for progression to fusion. Elife 3, e01879.